

Adsorption of Eu(III) onto Roots of Water Hyacinth

COLLEEN KELLEY,^{*,†}
 RANDALL E. MIELKE,[†]
 DARRYL DIMAQUIBO,[†]
 ABIGALE J. CURTIS,[†] AND
 JANE G. DEWITT[‡]

Departments of Chemistry, Northern Arizona University,
 Flagstaff, Arizona 86011-5698, and San Francisco State
 University, San Francisco, California 94132

The water hyacinth (*Eichhornia crassipes*) has drawn attention as a plant capable of removing pollutants, including toxic metals, from water. We are interested in the capacity of the water hyacinth to remediate aquatic environments that have been contaminated with the lanthanide metal, europium (Eu(III)). Using scanning electron microscopy (SEM) we have been able to determine that Eu(III) is adsorbed onto the surface of the roots from water and that the highest concentration of Eu(III) is on the root hairs. X-ray absorption spectroscopy (XAS) techniques were used to speciate the Eu(III) adsorbed onto the surface of the roots. The XAS data for Eu-contaminated water hyacinth roots provides evidence of a Eu–oxygen environment and establishes that Eu(III) is coordinated to 10–11 oxygen atoms at a distance of 2.44 Å. This likely involves binding of Eu(III) to the root via carboxylate groups and hydration of Eu(III) at the root surface.

Introduction

Environmental contamination of the aquatic environment by toxic metals is a serious problem (1). Unlike organic pollutants, toxic metals are not degradable by chemical or biological processes. Ideally, these contaminants should be remediated by concentrating them in a form convenient for reextraction, possible reuse, or at least proper disposal. Phytoremediation holds the potential of providing a sound alternative to current remediation strategies (2). We are interested in the capacity of an aquatic macrophyte, water hyacinth (*Eichhornia crassipes*), to remediate water that has been contaminated with lanthanide metals.

Water hyacinth was chosen for several reasons. Water hyacinth has been shown to accumulate high concentrations of toxic metals (3–8) and is currently being used to remediate sites contaminated with metals (9–13). In addition, these plants are easy to grow, propagate readily, and their large biomass facilitates handling and tissue manipulations.

We have chosen to study Eu(III) as a nonradioactive surrogate for trivalent actinides such as americium. Eu(III) has the same oxidation state, similar ionic radius, and similar coordination chemistry to Am(III) (14). Americium (III) is a significant component of ionic radioactive species found in liquid radioactive waste and has high radiotoxicity and a long half-life. Americium is present in the supernatant of

many of the Hanford waste tanks, and consequently the supernatant is considered high-level waste (15). Therefore, the adsorption of Eu(III) from an aquatic system onto the roots of water hyacinth provides an excellent model for the fate of Am(III) in the same system (16).

Removal of metal ions from solution by biomaterials is believed to occur through interactions with functional groups that are found in the proteins, lipids, and carbohydrates that make up the cell walls (17). It has been well established that carboxylate and sulfate groups are the dominant functional groups on the cell walls of *Datura innoxia* that bind Eu(III) (18–23). Previous investigations indicated that carboxyl and β -dicarbonyl groups are responsible for Eu³⁺ metal binding to *D. innoxia* above pH 3 (24). Measurements from Eu(III)-luminescence spectra have also indicated the possible formation of different binding modes between Eu³⁺ ions and carboxylates, including mono-, bi-, and tridentates (24). Sulfonates were reported to be involved in Eu³⁺ binding with more pronounced contributions at lower pH (i.e., <3) (24). Recent spectroscopic studies performed in our laboratory involving nuclear magnetic resonance (NMR) and infrared (IR) techniques have shown that carboxylate functionalities are also responsible for binding Eu(III) to the roots of water hyacinth (25). It is the aim of this investigation to determine: (1) the amount of Eu(III) bound to the roots of water hyacinth, (2) the location of the adsorbed Eu(III) (i.e., root surface, root hairs, etc.), and (3) the coordination environment of the adsorbed Eu(III). We have used scanning electron microscopy (SEM) to determine the location of Eu(III) bound to the roots and have used X-ray absorption spectroscopic (XAS) methods to determine its coordination environment.

The study of metal complexation to organic constituents and living organisms is a novel application of X-ray absorption spectroscopies (26–29). Salt et al. used this technique to determine the coordination sphere of intracellular cadmium in *Brassica juncea* seedlings (26, 27). More recently, Kramer et al. used XAS methods to determine the coordination chemistry of nickel in *Alyssum lesbiacum* (28).

Experimental Section

All chemicals were purchased from indicated sources and used without further purification.

Growth of Water Hyacinth. The water hyacinth, *Eichhornia crassipes*, was obtained from a local nursery and cultivated under aquatic greenhouse conditions (30). All plants were rinsed thoroughly with deionized, distilled water prior to investigation.

Contamination of Water Hyacinth with Eu(III). One healthy, mature water hyacinth plant was incubated for 48 hours in 2 L of 3.3×10^{-4} M solution of Eu(NO₃)₃·6H₂O (Aldrich) pH 3.5, and the experiment replicated eight times. Eight control plants were also incubated in deionized, distilled water for 48 hours.

Digestion of Water Hyacinth Plant Material in Preparation for Inductively Coupled Argon Plasma–Atomic Emission Spectroscopy (ICP–AES) Analyses. Contaminated plant material was dried at room temperature. Each individual plant was then divided into whole roots or leaves. Root and leaf material was ground to a fine powder with an electric grinder and digested in 100 mL water, 10 mL concentrated nitric acid, and 5 mL concentrated hydrochloric acid. Solutions were boiled until the total volume was reduced to 20 mL, then the samples were cooled, filtered, and the filtrate diluted to 100 mL with HPLC grade water. Digests were analyzed by ICP–AES methods using a JW38 instrument at Northern Arizona University. Quality control was enforced

* Corresponding author phone: (520) 523-7877; fax: (520) 523-8111; e-mail: colleen.kelley@nau.edu.

[†] Northern Arizona University.

[‡] San Francisco State University.

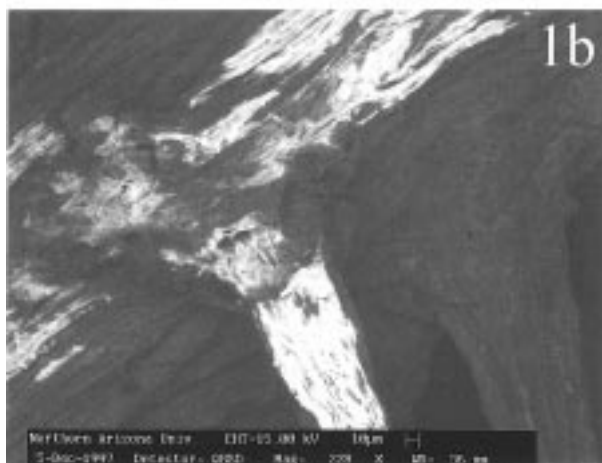
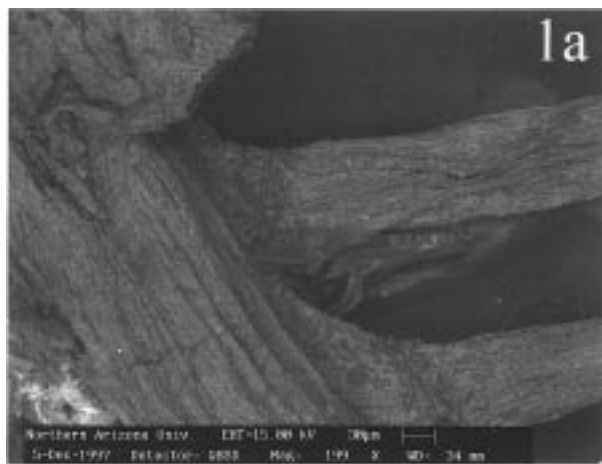


FIGURE 1. (1a) SEM micrograph of water hyacinth root. (1b) SEM micrograph of water hyacinth root incubated with Eu(III). The areas of fluorescence indicate the presence of Eu(III).

and instrumental accuracy was approximately $\pm 1.32 \times 10^{-5}$ M for Eu(III) concentration. Calibration checks with standard solutions (VWR) were performed every 10 samples.

Preparation of Roots of Water Hyacinth for SEM Analyses. Roots of contaminated water hyacinth (described above) were dried at room temperature and placed on aluminum stubs for analysis. SEM techniques were performed with a tungsten filament LEO 435 VP and Eu(III) was detected with a Quad Backscattering Detector (QBSD).

X-ray Absorption Spectroscopic (XAS) Investigation of Water Hyacinth Roots. Roots of water hyacinth exposed to Eu(III), as described above, were lyophilized prior to XAS measurements. Root material was ground in a mortar and pestle, packed into a 1 mm Al spacer with Kapton windows and frozen in liquid nitrogen. As a standard, solid $\text{Eu}(\text{NO}_3)_3 \cdot 6\text{H}_2\text{O}$ was diluted with boron nitride, ground to a fine powder, packed into a 1 mm Al spacer with Kapton windows, and frozen in liquid nitrogen. Eu L_3 -edge X-ray absorption spectra were measured on unfocused wiggler beamline 7-3 at the Stanford Synchrotron Radiation Laboratory under dedicated conditions (3 GeV, 50–100 mA). Energy monochromatization was achieved by using a Si (220) double-crystal monochromator detuned 50% at 7590 eV to minimize harmonic contamination with 1 mm high monochromator slits. Data were collected at 10 K, maintained by a continuous flow liquid helium cryostat (Oxford Instruments CF1208). Energy calibration was achieved using an internal Eu foil standard with the first inflection point assigned as 6979 eV (31). The fluorescent signal was measured using a 13 element Ge array detector (32) (Canberra) windowed on the Eu $L\alpha$ signal (6059

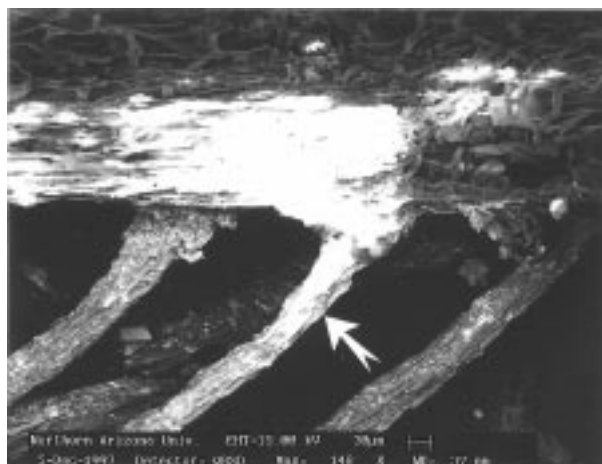


FIGURE 2. SEM micrograph of water hyacinth root incubated with Eu(III). The arrow denotes the higher concentration of Eu(III) found on the root hairs.

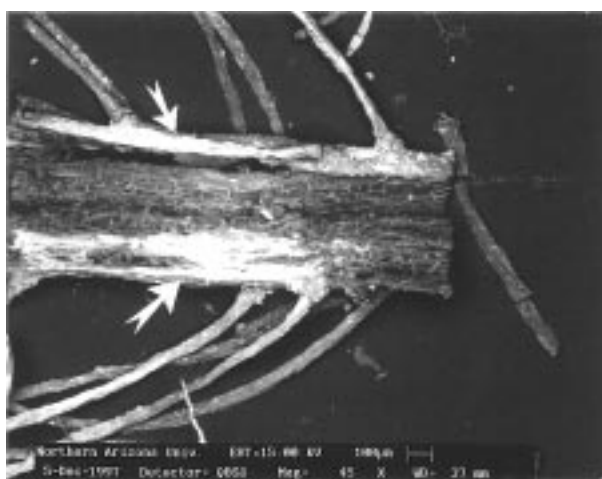


FIGURE 3. SEM micrograph of a cross-section of a water hyacinth root incubated with Eu(III). The arrows indicate that the Eu(III) is found on the surface of the root.

eV). Extended X-ray absorption fine spectroscopy (EXAFS) data were collected to $k = 12.5 \text{ \AA}^{-1}$, terminating at the Eu L_2 -edge. Two scans were averaged for the $\text{Eu}(\text{NO}_3)_3 \cdot 6\text{H}_2\text{O}$ and the Eu-bound hyacinth root samples. Standard methods of data reduction and analysis were performed (33, 34) using the EXAFSPAK suite of programs developed by G. George of SSRL. Nonlinear least-squares curve-fitting techniques to the raw k^3 -weighted EXAFS data were done using curved-wave amplitude and phase parameters tabulated by McKale (35). For the fits, coordination number (N) and energy offset (EO) were fixed and the distance (R) and Debye–Waller factor (σ^2) were allowed to float. Using these techniques, errors of approximately 25% in the coordination number and 0.02 \AA in the distance were typical (33, 34).

Results and Discussion

Determination of the Amount of Eu(III) Adsorbed Onto Roots of Water Hyacinth. Twenty-six percent (8.7×10^{-5} mol Eu(III)/g dry root material from an initial solution of 3.3×10^{-4} M Eu(III)) of the Eu(III) in the contaminant solution was removed, and essentially all of the removed Eu(III) is found in the root material. This result is significant in that it is the first step toward determining whether a water hyacinth system presents a viable remediation strategy for the lanthanide metals and, more importantly, the trivalent radioactive actinides such as Am(III). The accumulation of

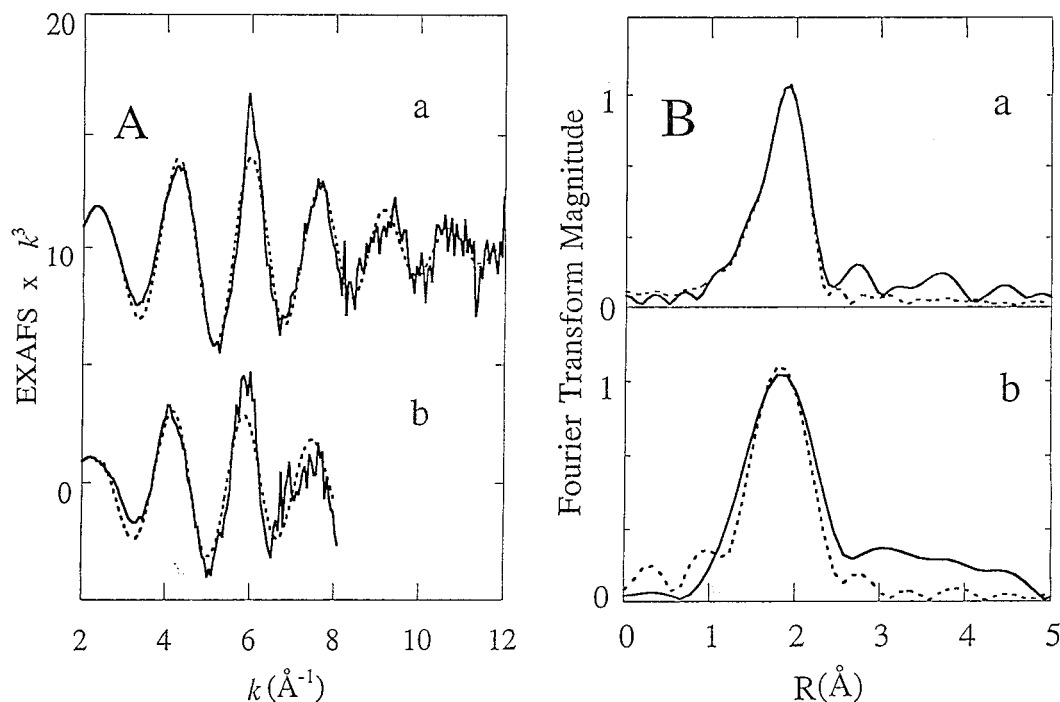


FIGURE 4. Eu L3-edge EXAFS data (A) and Fourier transforms of the EXAFS data (B) for water hyacinth (a) and $\text{Eu}(\text{NO}_3)_3 \cdot 6\text{H}_2\text{O}$ (b) along with fits to the data. The solid line is the data and the dashed line is the fit to the data (fits presented in Table 1) in both A and B.

$\text{Eu}(\text{III})$ on roots of water hyacinth is of the same order of magnitude as predicted for $\text{Eu}(\text{III})$ accumulation by *D. innoxia* at pH 3.5 (24), and these results are in agreement with the results that have been reported for the removal of other metals from solution by roots of water hyacinth (3–13).

SEM Micrographs. We used SEM techniques to image $\text{Eu}(\text{III})$ on water hyacinth roots. SEM allows for localization of $\text{Eu}(\text{III})$ by detection of backscattered electrons (BSE) using a quad backscattering detector (QBSD). The net result of BSE–QBSD is an illumination of $\text{Eu}(\text{III})$ present in the sample.

Roots of water hyacinth that have been contaminated with $\text{Eu}(\text{III})$ are shown in Figures 1, 2, and 3. These micrographs clearly show that $\text{Eu}(\text{III})$ is concentrated on the external surface of the roots, with the most fluorescence, hence, highest concentration of $\text{Eu}(\text{III})$, located on the hairs of the root (Figure 2). A cross-section of a root confirms that $\text{Eu}(\text{III})$ is concentrated on the external surface of the root (Figure 3). For comparison, a similar view of a roots of water hyacinth that have not been contaminated with $\text{Eu}(\text{III})$ is shown in Figure 1a.

XAS Investigation of $\text{Eu}(\text{III})$ on the Roots of Water Hyacinth. It has been established by NMR and IR spectroscopy that carboxylate groups are the dominant functional groups responsible for binding $\text{Eu}(\text{III})$ to the roots of water hyacinth (25). X-ray absorption spectroscopy (XAS) enabled the determination of the $\text{Eu}(\text{III})$ coordination environment on roots of water hyacinth.

The EXAFS data and the Fourier transforms of the data from 2.5 to 12.0 \AA^{-1} for the $\text{Eu}(\text{III})$ -water hyacinth sample and from 2.5 to 8.0 \AA^{-1} for the $\text{Eu}(\text{NO}_3)_3 \cdot 6\text{H}_2\text{O}$ data show that the coordination environment for $\text{Eu}(\text{III})$ is similar in both samples (Figure 4). The $\text{Eu}(\text{III})$ environment in $\text{Eu}(\text{NO}_3)_3 \cdot 6\text{H}_2\text{O}$ consists of three bidentate NO_3^- groups and four H_2O molecules resulting in a coordination of 10 oxygen atoms at an average distance of 2.48 \AA (36). Fits to the EXAFS data for $\text{Eu}(\text{NO}_3)_3 \cdot 6\text{H}_2\text{O}$ are in excellent agreement with this structure (Table 1), with the best fit to the data corresponding to 10 oxygen atoms at an average distance of 2.48 \AA . For the $\text{Eu}(\text{III})$ -water hyacinth roots, equally good fits to the data were

TABLE 1. Results of Fits to the EXAFS Data

	N^c	R (\AA)	σ^2 (\AA^2)	EO (eV)	F
$\text{Eu}(\text{NO}_3)_3 \cdot 6\text{H}_2\text{O}^a$	10 O	2.48 (1)	0.01 (2)	-5.027	0.713
hyacinth root ^b	11 O	2.44 (1)	0.011 (1)	-5.027	0.520

^a Data fit over a range of 2.5–8.0 \AA^{-1} . ^b Data fit over a range of 2.5–12.0 \AA^{-1} . ^c Goodness of fit, $F = \sum[(\chi_{\text{exp}} - \chi_{\text{fit}})k^6]^2/n$ where n = number of points. The estimated error is reported in parentheses for R and σ^2 .

obtained with 10 or 11 oxygen atoms at a slightly shorter $\text{Eu}-\text{O}$ distance of 2.44 \AA . The data and the fits to the data are presented in Figure 4. On average, $\text{Eu}-\text{O}$ bond lengths with bidentate ligands are longer than $\text{Eu}-\text{O}$ bond lengths with water (36). A shorter average $\text{Eu}-\text{O}$ bond length for the hyacinth sample compared to the $\text{Eu}-\text{O}$ bond length in $\text{Eu}(\text{NO}_3)_3 \cdot 6\text{H}_2\text{O}$ may therefore reflect $\text{Eu}(\text{III})$ coordination by fewer carboxylate groups and more water molecules. The $\text{Eu}(\text{NO}_3)_3 \cdot 6\text{H}_2\text{O}$ EXAFS data was impacted by the presence of monochromator glitches at $k = 8 \text{\AA}^{-1}$ and the presence of Fe in the Be window in the beamline. The fluorescence data for $\text{Eu}(\text{NO}_3)_3 \cdot 6\text{H}_2\text{O}$ was unusable beyond the $k = 8 \text{\AA}^{-1}$ glitch. Although the $k = 8 \text{\AA}^{-1}$ can also be seen in the $\text{Eu}(\text{III})$ -water hyacinth data, its impact was much less severe and the data were usable over the entire data range collected.

Fits were also attempted using nitrogen amplitude and phase parameters, though EXAFS has a limited capacity to discriminate between atoms of similar backscattering sizes. While reasonable fits to the data were obtained with nitrogen, the coordination numbers were unreasonably high. For example, the best nitrogen fit to the $\text{Eu}(\text{NO}_3)_3 \cdot 6\text{H}_2\text{O}$ consisted of 12 N atoms at 2.45 \AA , but no more than 3 nitrogen atoms are available to coordinate $\text{Eu}(\text{III})$ in this compound. Additionally, the $\text{Eu}-\text{N}$ bond length is shorter than the typical $\text{Eu}-\text{N}$ bond lengths reported for a number of model compounds (2.6–2.8 \AA) (37–41). A $\text{Eu}-\text{O}$ coordination environment on the hyacinth roots is more reasonable than a $\text{Eu}-\text{N}$ coordination environment because of the high content of carboxylate groups from organic acids present on the surface of water hyacinth roots (25, 42). Therefore, although nitrogen amplitude and phase parameters can fit

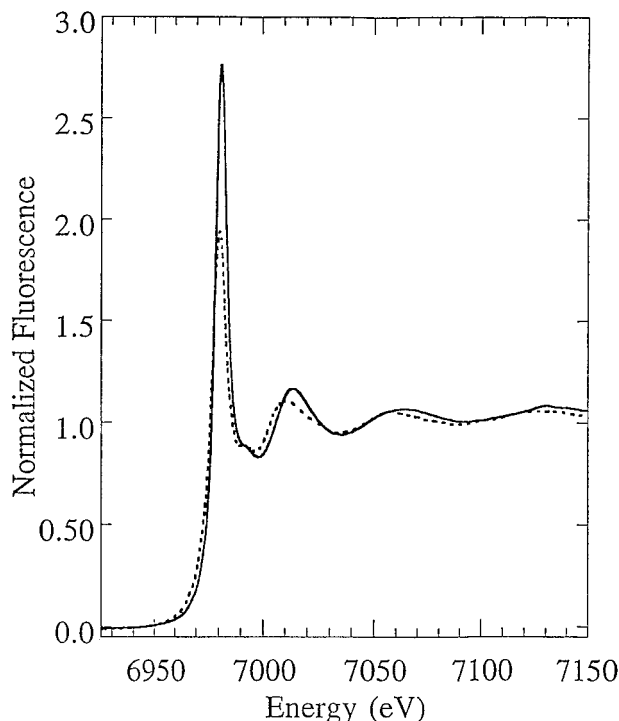


FIGURE 5. Eu L₃-edge near-edge spectra for Eu(III)-water hyacinth (solid line) and Eu(NO₃)₃·6H₂O (dashed line). The difference in intensity and position of the transition at ~6980 eV could be attributed to mixture of 1:1 and 1:2 Eu(III)/carboxylate binding ratios found between Eu(III) and the carboxylates on the roots of water hyacinth.

the EXAFS data mathematically, we have rejected these results because they are chemically unreasonable.

The Eu L₃-edge spectra for the Eu(III)-water hyacinth and Eu(NO₃)₃·6H₂O data is presented in Figure 5. A slight shift to higher energy is seen in the position of the edge for the Eu(III)-water hyacinth data (inflection at 6981.2 eV) compared to the Eu(NO₃)₃·6H₂O data (inflection at 6980.7 eV). Additionally, the intensity of the edge feature is greater for the Eu(III)-water hyacinth samples than for the Eu(NO₃)₃·6H₂O sample. This difference may reflect a somewhat more ionic europium environment on the surface of the water hyacinth roots compared to the environment in europium nitrate.

The data presented in this paper have enabled the speciation of Eu(III) on the roots of water hyacinth to be determined. This has important environmental implications in that (1) it provides an excellent model for the speciation of trivalent radioactive actinides such as Am(III) in the same system, and (2) while other environmental conditions may change (pH, the presence of other metal ions, the presence of humic/fulvic acids, etc.), the speciation of the adsorbed Eu(III) on roots of water hyacinth will not change. These studies established a baseline for the intrinsic interaction between Eu(III) and roots of water hyacinth. The anticipated complexity of a system such as the Hanford waste tanks containing Am(III) in the supernatant requires the elimination of variables in a systematic way so that true factors influencing Eu(III) or Am(III) removal can be identified. We have established the speciation of Eu(III) in our water hyacinth system and are now poised to model more complex systems contaminated with Am(III) using Eu(III) as a metal surrogate.

Acknowledgments

This work was funded in part by the Department of Energy through the Historically Black Colleges and Universities/Minority Institutions Environmental Technology Consortium.

X-ray absorption spectroscopic work was done at SSRL which is operated by the Department of Energy, Office of Basic Energy Sciences. The SSRL Biotechnology Program is supported by the NIH, Biomedical Research Technology Program, National Center for Research Resources. Further support is provided by the Department of Energy, Office of Health and Environmental Research. We would also like to thank Marilee Sellers and Lawrence Fritz (N.A.U.) for their assistance in acquiring the SEM micrographs.

Literature Cited

- (1) Forstner, U.; Wittmann, G. T. W. *Metal Pollution in the Aquatic Environment*, Springer, Berlin, 1979.
- (2) Salt, D. E.; Smith, R. D.; Raskin, I. *Annu. Rev. Plant. Physiol. Plant Mol. Biol.* **1998**, *49*, 643–668.
- (3) O'Keeffe, O. H.; Hardy, J. K.; Rao, R. A. *Environ. Pollut. Ser. A* **1984**, *34*, 133–147.
- (4) Lee, T. A.; Hardy, J. K. *J. Environ. Sci. Health A* **1987**, *22*, 141–160.
- (5) Low, K. S.; Lee, C. K. *Pertanika* **1990**, *13*, 129–131.
- (6) Hao, Y.; Roach, A. L.; Ramelow, G. J. *J. Environ. Sci. Health* **1993**, *A28*, 2333–2343.
- (7) Delgado, M.; Bigeriego, M.; Guardiola, E. *Water Res.* **1993**, *27*, 269–272.
- (8) Low, K. S.; Lee, C. K.; Tai, C. H. *J. Environ. Sci. Health* **1994**, *A29*, 171–188.
- (9) Wolverton, B. C. *NASA Technol. Mem.* **1975**, TMX-72721.
- (10) Chigno, F. E.; Smith, R. W.; Shore, F. L. *Environ. Pollut. Ser. A* **1982**, *27*, 31–36.
- (11) Muramoto, S.; Oki, Y. *Bull. Environ. Contam. Toxicol.* **1983**, *30*, 170–177.
- (12) Gonzalez, H.; Lodenius, M.; Otero, M. *Bull. Environ. Contam. Toxicol.* **1989**, *43*, 910–914.
- (13) Watanabe, M. E. *Environ. Sci. Technol.* **1997**, *31*, 182–186.
- (14) Cotton, F. A.; Wilkinson, G. *Advanced Inorganic Chemistry*, 5th ed.; John Wiley & Sons: New York, 1988.
- (15) Norton, M. V.; DiGiano, F. A.; Hallen, R. T. *Water Environ. Res.* **1997**, *69*, 244–253.
- (16) Ephraim, J. H. *Sci. Total Environ.* **1991**, *108*, 261–273.
- (17) Green, B.; Hosea, M.; McPherson, R.; Henzl, M.; Alexander, M. D.; Darnall, D. W. *Environ. Sci. Technol.* **1986**, *20*, 627–632.
- (18) Ke, H.-Y. D.; Birnbaum, E. R.; Darnall, D. W.; Rayson, G. D.; Jackson, P. J. *J. Appl. Spectrosc.* **1992**, *46*, 479–488.
- (19) Ke, H.-Y. D.; Birnbaum, E. R.; Darnall, D. W.; Rayson, G. D.; Jackson, P. J. *Environ. Sci. Technol.* **1992**, *26*, 782.
- (20) Ke, H.-Y. D.; Rayson, G. D.; Jackson, P. J. *Environ. Sci. Technol.* **1993**, *27*, 2466.
- (21) Ke, H.-Y. D.; Anderson, W. L.; Moncrief, R. M.; Rayson, G. D.; Jackson, P. J. *Environ. Sci. Technol.* **1994**, *28*, 586.
- (22) Drake, L. R.; Lin, S.; Rayson, G. D.; Jackson, P. J. *Environ. Sci. Technol.* **1996**, *30*, 110.
- (23) Rayson, G. D.; Lin, S. *Environ. Sci. Technol.* **1998**, *32*, 1488–1493.
- (24) Drake, L. R.; Hensman, C. E.; Lin, S.; Rayson, G. D.; Jackson, P. J. *J. Appl. Spectrosc.* **1997**, *51*, 1476.
- (25) Kelley, C.; Curtis, A. J.; Uno, J. K.; Berman, C. L. *Water, Air, Soil Pollut.* Accepted for publication.
- (26) Salt, D. E.; Prince, R. C.; Pickering, I. J.; Raskin, I. *Plant Physiol.* **1995**, *109*, 1427.
- (27) Salt, D. E.; Pickering, I. J.; Prince, R. C.; Gleba, D.; Dushenkov, S.; Smith, R. D.; Raskin, I. *Environ. Sci. Technol.* **1997**, *31*, 1636.
- (28) Kramer, U.; Cotter-Howells, J. D.; Charnock, J. M.; Baker, A. J. M.; Andrew, C.; Smith, J. *Nature* **1996**, *379*, 635–638.
- (29) Denecke, M. A.; Pompe, S.; Reich, T.; Moll, H.; Bubner, M.; Heise, K. H.; Nicolai, R.; Nitsche, H. *Radiochim. Acta* **1997**, *79*, 151–159.
- (30) Nir, R.; Gasith, A.; Perry, A. S. *Bull. Environ. Contam. Toxicol.* **1990**, *44*, 149–157.
- (31) Scott, R. A.; Hahn, J. E.; Doniach, S.; Freeman, H. C.; Hodgson, K. O. *J. Am. Chem. Soc.* **1982**, *104*, 5364–5369.
- (32) Cramer, S. P.; Tench, O.; Yocum, M.; George, G. N. *Nucl. Instrum. Methods Phys. Res.* **1988**, *A266*, 586–591.
- (33) Scott, R. A. *Methods Enzymol.* **1985**, *117*, 414–459.
- (34) Koningsberger, D. C.; Prins, R. *X-ray Absorption. Principles, Applications and Techniques of EXAFS, SEXAFS and XANES*; John Wiley and Sons: New York, 1988.
- (35) McKale, A. G.; Veal, B. W.; Paulikas, A. P.; Chan, S.-K.; Knapp, G. S. *J. Am. Chem. Soc.* **1988**, *110*, 3763–3768.

- (36) On the basis of X-ray powder diffraction data, $\text{Eu}(\text{NO}_3)_3 \cdot 6\text{H}_2\text{O}$ has the same structure as $\text{Tb}(\text{NO}_3)_3 \cdot 6\text{H}_2\text{O}$. Moret, E.; Bünzli, J.-C. G.; Schenk, K. J. *Inorg. Chim. Acta* **1990**, *178*, 83–85.
- (37) Zhuravlev, M. G.; Sergeev, A. V.; Mistryokov, V. E.; Mikhailov, Y. N.; Shchelokov, R. N. *Dokl. Akad. Nauk SSSR* **1989**, *306*, 878–883.
- (38) Bombieri, G.; Benetollo, F.; Polo, A.; De Cola, L.; Hawkins, W. T.; Vallarino, L. M. *Polyhedron* **1989**, *8*, 2157–2167.
- (39) Bombieri, G.; Benetollo, F.; Polo, A.; Fonda, K. K.; Vallarino, L. M. *Polyhedron* **1991**, *10*, 1385–1394.
- (40) Nakamura, K.; Kurisaki, T.; Wakita, H.; Yamaguchi, T. *Acta Crystallogr.* **1995**, *C51*, 1559–1563.
- (41) Liu, S.-Y.; Maunder, G. H.; Sella, A.; Stevenson, M.; Tocher, D. A. *Inorg. Chem.* **1996**, *35*, 76–81.
- (42) Low, K. S.; Lee, C. K.; Tan, K. K. *Bioresour. Technol.* **1995**, *52*, 79–83.

Received for review July 28, 1998. Revised manuscript received November 30, 1998. Accepted February 17, 1999.

ES9807789